DOI: 10.1002/ejic.201001106

Ring-Shaped *J*-Type and Star-Shaped *H*-Type Nanostructures of an Unsymmetrical (Phthalocyaninato)zinc Complex

Naichang Tian,[a] Pan Ma,[a] Quanbo Wang,[a] Xianyao Zhang,[a] Jianzhuang Jiang,*[a,b] and Ming Bai*[c]

Keywords: Phthalocyanines / Self-assembly / Nanostructures / Aggregation

Unsymmetrical (phthalocyaninato)zinc complex **1** was synthesized by transesterification and self-assembled into ring-shaped nanostructures with *J*-type aggregation at the chloroform/water interface and into star-shaped nanostructures with *H*-type aggregation in the chloroform/methanol system, respectively. Its self-assembly properties have been studied by spectroscopic, transmission electron microscopy (TEM), scanning electron microscopy (SEM), and X-ray diffraction (XRD) techniques. The star-shaped nanostructures were found to have better semiconducting properties than the ring-shaped nanostructures due to the more effective intermolecular π-electron delocalization. The results appear to represent the first example of nanostructures with *J*- and *H*-type molecular conformations self-assembled from the same phthalocyanine compound in different solvent systems with novel ring- and star-shaped morphologies, respectively.

Introduction

In recent years, considerable attention has been directed towards the construction of supramolecular assemblies with well-defined nanoscale dimensions.[1,2] In particular, the self-assembly of functional organic molecules into well-defined organized structures has attracted considerable research interest due to their versatile applications in nanoscience and nanotechnology.[3,4] Self-assembly is a natural and spontaneous process that mainly depends on noncovalent interactions such as π–π, van der Waals, hydrogen-bonding, hydrophilic/hydrophobic, and electrostatic interactions as well as metal–ligand coordination bonding. A variety of artificial self-assembled organic nanostructures with the morphology of fibers,[5] ribbons,[6] particles,[7] tubes,[8] and vesicles[9] have been prepared from different molecular materials. However, unlike their inorganic counterparts, relatively few organic nanostructures with ring- and star-shaped morphologies, in particular those prepared by the self-assembly method, have been reported.[10]

Owing to their biological importance, porphyrin derivatives have attracted significant research interest. However, their structural analogues, phthalocyanine compounds, have been studied even more intensively due to their high stability and useful catalytic, chemical-sensing, and optical-limiting properties.[11] In nature, the ring-shaped assemblies of porphyrins in the bacterial light-harvesting complex LH2 are known to be responsible for the absorption of light and the storage and transportation of light energy to the reaction center.[10a] A series of synthetic porphyrin derivatives have been self-assembled into micrometer-scale rings by a simple method.[10b] However, there still appears to be no reports on self-assembled star-shaped nanostructures of porphyrin derivatives. This also seems true for the phthalocyanine compounds despite the fabrication of various kinds of phthalocyanine nanostructures with different morphologies.[12–14] In fact, nanoscale or even microscale assemblies with ring-shaped morphology have not been reported for phthalocyanine derivatives thus far.

In this paper we report the synthesis and spectroscopic characterization of unsymmetrical (phthalocyaninato)zinc complex **1** (Scheme 1). In particular, this compound was elaborated into novel ring-shaped nanostructures at the interface of a chloroform/water solvent system and into star-shaped nanostructures in the mixed solvent of chloroform/methanol, thereby revealing the effect of the solvent system on the intermolecular interaction and in turn on the molecular packing mode, morphology, and dimensions of self-assembled nanostructures. The star-shaped nanostructures with *H*-type aggregation were revealed to have better semiconducting properties than the ring-shaped nanostructures with *J*-type aggregation due to a more effective intermolecular π-electron delocalization.

[a] Department of Chemistry, Shandong University, Jinan 250100, China
Fax: +86-531-856-5211
E-mail: jzjiang@sdu.edu.cn
jianzhuang@ustb.edu.cn
[b] Department of Chemistry, University of Science and Technology Beijing, Beijing 100083, China
[c] Marine College, Shandong University at Weihai, Weihai 264209, China
E-mail: ming_bai@sdu.edu.cn

Supporting information for this article is available on the WWW under http://dx.doi.org/10.1002/ejic.201001106.

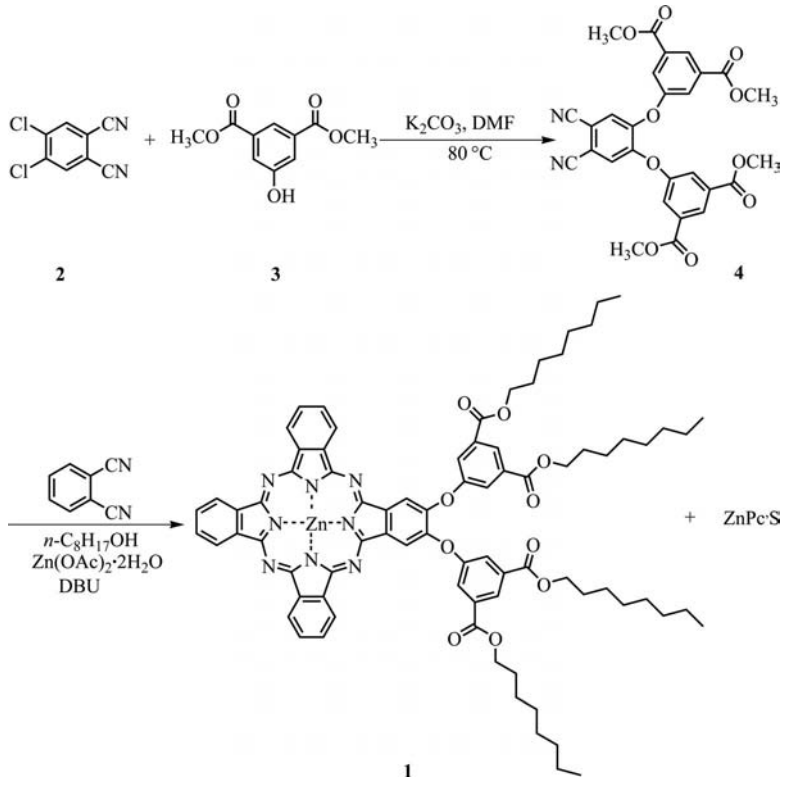

Scheme 1. Synthesis of unsymmetrical (phthalocyaninato)zinc complex **1**.

Results and Discussion

Synthesis

As shown in Scheme 1, the aromatic nucleophilic substitution reaction between 4,5-dichlorophthalonitrile (**2**) and dimethyl 5-hydroxyisophthalate (**3**) gave 4,5-bis[3,5-bis-(methoxycarbonyl)phenoxy]phthalonitrile (**4**),[15] which underwent mixed cyclic tetramerization with phthalonitrile to provide the target unsymmetrical (phthalocyaninato)zinc complex **1** in relatively good yield in addition to other species of symmetrical and unsymmetrical (phthalocyaninato)-zinc complexes. A satisfactory elemental analysis was obtained for the unsymmetrical (phthalocyaninato)zinc compound after repeated column chromatography and recrystallization. This compound was also characterized by a wide range of spectroscopic methods including ^{1}H NMR (Figure S1, Supporting Information), electronic absorption, and IR spectroscopy and by MALDI-TOF mass spectrometry (Figure S2, Supporting Information).

Electronic Absorption Spectra

The electronic absorption spectrum of the unsymmetrical (phthalocyaninato)zinc complex **1** in $CHCl_3$ was recorded and the data are compiled in Table S1 (Supporting Information) and Figure 1. As expected, the spectrum of this compound shows the typical features of a (phthalocyaninato)metal complex, revealing its nonaggregated nature in $CHCl_3$. In line with other (phthalocyaninato)metal compounds,[16] the absorption at around 344 nm for **1** can be attributed to the phthalocyanine Soret band, whereas the absorption at 672 nm with the vibrational shoulder at 607 nm to the Q band. The electronic absorption spectra of the aggregates formed by **1** at the chloroform/water interface and in the mixed solvent chloroform/methanol are also displayed in Figure 1 and are significantly different to the spectrum of the same compound dissolved in $CHCl_3$. Clear band-broadening is observed as a result of the significant intermolecular interactions in the self-assembled nanostructures. In comparison with the chloroform solution spectrum, the main phthalocyanine Q absorption of the nanostructures formed at the chloroform/water interface (see Figure 4A and B) is redshifted to 680 nm, which indicates the formation of *J*-type aggregates during the self-assembly process of **1** at the chloroform/water interface.[17] In contrast, the main phthalocyanine Q band of the nanostructures formed in the chloroform/methanol system is blue-shifted relative to that in chloroform solution to 666 nm, which indicates the formation of *H*-type aggregates during the self-assembly process in the mixed chloroform/methanol solvent. In particular, a new band emerges at around 753 nm in the electronic absorption spectrum of star-shaped nanostructures. In fact, a pronounced additional absorption band emerging at a longer wavelength is typically a sign of an effective π–π interaction in the cofacial configuration of molecular stacking.[6,18] A similar phenomenon has also been observed with perylenetetracarboxylic diimide (PTCDI) compounds.[6b] The different self-assembly

behavior of this unsymmetrical (phthalocyaninato)zinc compound **1** in different solvent systems, as indicated by electronic absorption spectroscopy, reveals the effect of the solvent–phthalocyanine molecular interaction during the self-assembly process, which counterbalances the phthalocyanine intermolecular interaction, in particular, the hydrophobic interaction between side-chains, on the molecular packing mode. Further evidence for this is provided from X-ray diffraction (XRD) results as detailed below.

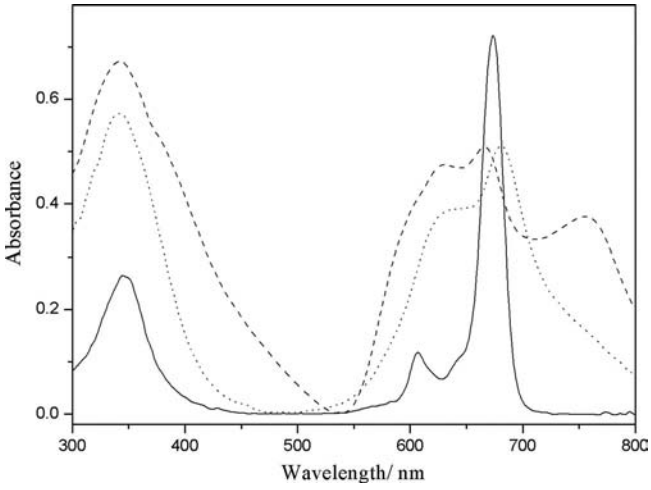

Figure 1. Electronic absorption spectra of **1** in chloroform (1×10^{-5} mol L^{-1}, solid line), self-assembled nanostructures of **1** formed at the chloroform/water interface as a film (1×10^{-3} mol L^{-1}, dotted line) and nanostructures dispersed in methanol (1×10^{-3} mol L^{-1}, dashed line).

X-ray Diffraction Patterns of the Nanostructures

The internal structures of self-assembled nanostructures were further investigated by X-ray diffraction (XRD). Figure 2 exhibits the diffraction patterns of the self-assembled nanostructures formed from **1**. As can be seen from Figure 2A, the XRD diagram of the nanostructures formed at the chloroform/water interface shows a strong refraction peak at $2\theta = 3.17°$ (corresponding to 2.79 nm), ascribed to refraction from the (100) plane. This value is about 10% shorter than the total length of the molecule of **1** along the long axis, 3.10 nm, obtained from the energy-optimized conformation of the molecule by DFT calculation at the B3LYP/6-31G(d) level of theory (Scheme S1, Supporting Information). Based on this result and in combination with the electronic absorption spectrum of the nanostructures formed at the chloroform/water interface, this is probably due to the edge-on orientation[19] (which suggests that the long axes of the molecules are tilted to some extent away from the substrate plane, which is a common structural motif in organic semiconductor thin films) and face-to-face stacking occurring in the phthalocyanine molecules, in line with strong hydrophobic interactions between side-chains of neighboring (phthalocyaninato)zinc molecules, which results in effective side-chain interdigitation and leads to a shortened length along the longitudinal direction (Figure 3A).[6b,20] In addition, the XRD pattern displays one well-defined peak at the wide-angle range corresponding to a distance of 0.42 nm, which is related to the liquid-like order of the alkyl chains.[21] The other two peaks at 2θ = 28.10 and 28.94° (corresponding to 0.32 and 0.31 nm) are associated with π–π stacking of neighboring phthalocyanine rings along the direction perpendicular to the phthalocyanine rings[22] and dialkyl ester phenyl rings between the adjacent molecules and/or in the same molecule, respectively. A schematic representation of the ordering of **1** at the chloroform/water interface is shown in Figure 3A.

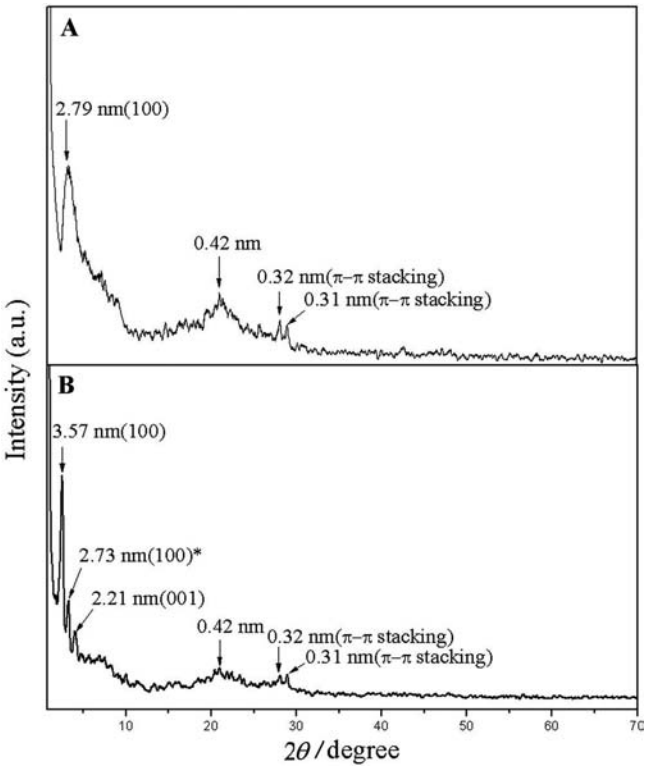

Figure 2. X-ray powder diffraction patterns of nanostructures of compound **1** formed (A) at the chloroform/water interface and (B) in the chloroform/methanol system.

As shown in Figure 2B, the XRD diagram of the nanostructures formed in the chloroform/methanol solvent system shows three strong peaks at 2θ = 2.47, 3.24, and 4.00° (corresponding to 3.57, 2.73, and 2.21 nm), which are ascribed to refractions from the (100), (100)*, and (001) planes. Note that for the nanostructures of **1** formed in the chloroform/methanol system, the refraction peak at 2.73 nm is almost the same as that at 2.79 nm detailed above, which indicates that the aggregation behavior at the chloroform/water interface also partially exists under these conditions. However, another two strong Bragg diffractions appear at 3.57 and 2.21 nm, which implies a different molecular stacking mode of compound **1** in the chloroform/methanol system compared with in the chloroform/water system. By analyzing these XRD data in combination with the experimental electronic absorption spectra and the sim-

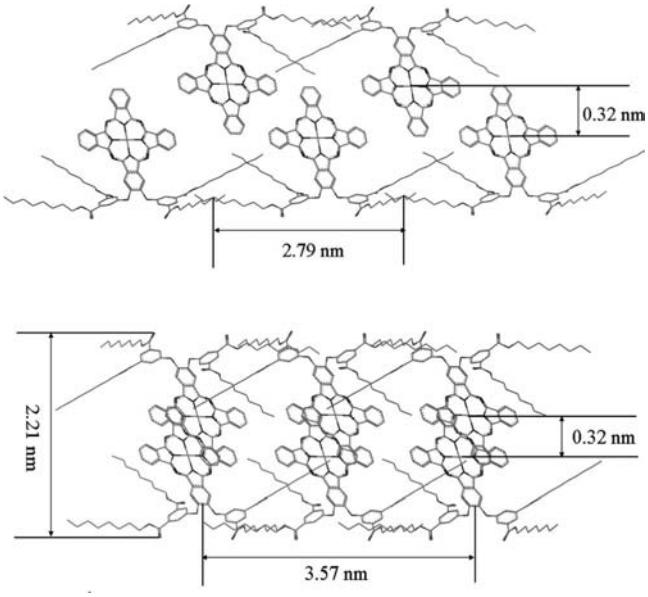

Figure 3. Schematic representation of the unit cell of (A) the ring-shaped nanostructures formed from **1** at the chloroform/water interface and (B) the star-shaped nanostructures formed from **1** in the chloroform/methanol system.

ulated molecular dimensions of **1** shown in Scheme S1 (Supporting Information), we can propose that in the chloroform/methanol system a dimeric supramolecular structure is formed in the first stage during the molecular self-assembly process of this compound, which depends mainly on the π–π interaction between two overlapped phthalocyanine cores of compound **1**, and this further self-assembles into the target nanostructures by side-chain interdigitation between adjacent dimeric supramolecular structures. A two-dimensional order is observed in which the cell parameter of 2.21 nm originates from the π–π stacking of neighboring, cofacially stacked phthalocyanine cores, and the large cell parameter of 3.57 nm arises from three dimeric supramolecular structures formed by side-chain interdigitation of compound **1** (Figure 3B). In the wide-angle region, peaks at 0.42, 0.32, and 0.31 nm are also observed, as was the case for the nanostructures formed at the chloroform/water interface.

Aggregate Morphology

The morphologies of the aggregates were examined by scanning electron microscopy (SEM) and transmission electron microscopy (TEM; Figure 4). As can be seen in Figure 4A and B, depending mainly on intermolecular π–π interactions in cooperation with van der Waals interactions, compound **1** self-assembles into nanostructures with a ring-shaped morphology with the outer diameter of the rings in the range of 1.35–1.83 μm and the average width of the bands of the rings varying between 110 and 140 nm at the chloroform/water interface. The formation of such ring-shaped nanostructures is attributed to the presence of gas bubbles in solution resulting from a complicated process determined by hydrodynamic and surface effects.[10b,23] In the present system, gas bubbles were formed when the chloroform was vaporized from the sample because chloroform is not soluble in water.

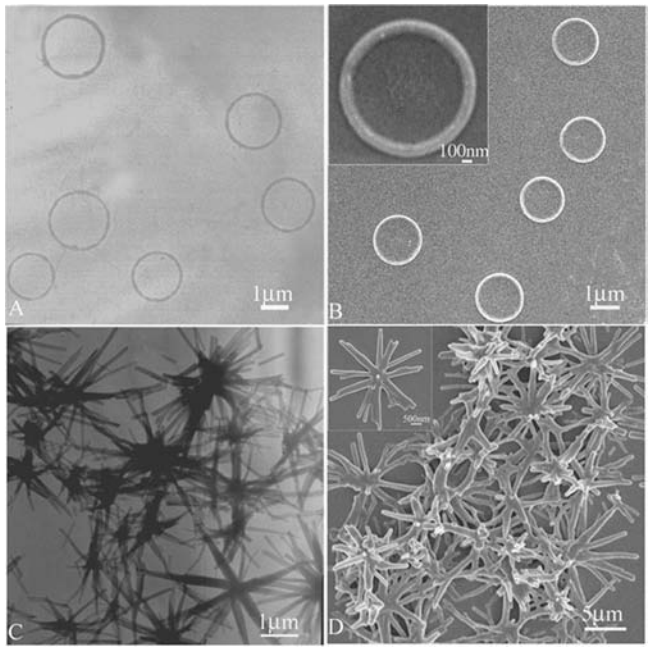

Figure 4. Ring-shaped nanostructures self-assembled from **1** at the chloroform/water interface observed by (A) TEM and (B) SEM and star-shaped nanostructures formed from **1** in the chloroform/methanol system observed by (C) TEM and (D) SEM.

As shown in Figure 4C and D, in the chloroform/methanol solvent system, depending again mainly on intermolecular π–π and van der Waals interactions, compound **1** self-assembles into nanostructures with a star-shaped morphology several micrometers in length and with a width of around 300–400 nm. In addition, we have proposed a schematic representation of the supramolecular structure of the star-shaped nanostructures with *H*-type aggregation based on electronic absorption and XRD analysis results.

FTIR Spectra

The FTIR spectra of the unsymmetrical (phthalocyaninato)zinc complex **1** and its self-assembled nanostructures are shown in Figure S3 (Supporting Information). The IR spectra of the nanostructures and **1** share similar features, which unambiguously confirms the nanostructures to be composed of the corresponding phthalocyanine compound **1**. The absorption at 1724 cm^{-1} in the IR spectrum of **1** is clearly due to the C=O vibration,[24] which appears at 1726 cm^{-1} for the self-assembled ring- and star-shaped nanostructures. The absorptions at 2923 and 2853 cm^{-1} in the IR spectrum of **1** are due to CH_2 antisymmetric and symmetric stretching vibrations of the side-chains.[25] These

vibrations give counterpart absorptions at 2926 and 2855 cm^{-1} for the ring-shaped nanostructures and at 2923 and 2853 cm^{-1} for the star-shaped nanostructures.

I–V Properties

To investigate the semiconducting properties of this phthalocyanine complex, the current–voltage characteristics of the two kinds of nanostructures of the unsymmetrical (phthalocyaninato)zinc complex **1** were recorded (Figure 5). The conductivities of the ring- and star-shaped nanostructures extracted from the quasi-linear region at low bias (up to 0 V) are around 5.6×10^{-6} and 1.5×10^{-5} $S\,m^{-1}$, respectively, which indicates that the star-shaped nanostructures with *H*-type aggregation have a better semiconducting ability than the ring-shaped nanostructures with *J*-type aggregation for this phthalocyanine derivative. This is mainly due to more effective intermolecular π-electron delocalization in the star-shaped nanostructures, which favors charge migration and leads to the enhancement in current.[26]

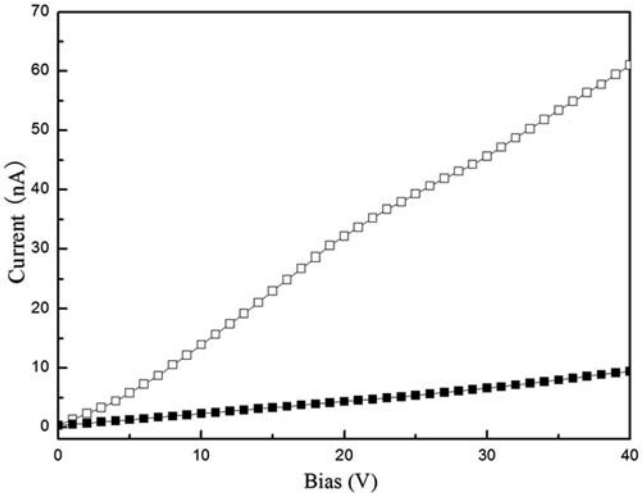

Figure 5. *I–V* curves measured for ring-shaped (filled squares) and star-shaped (empty squares) nanostructures of the unsymmetrical (phthalocyaninato)zinc complex **1**.

Conclusions

Unsymmetrical (phthalocyaninato)zinc complex **1** with low molecular symmetry decorated with octyl ester chains linked to the phthalocyanine ring and synthesized by transesterification was successfully elaborated into *J*- and *H*-type nanostructures with ring- and star-shaped morphologies, respectively, in different solvent systems for the first time, revealing the effect of solvent system on the intermolecular interactions and in turn on the molecular packing mode, morphologies, and dimensions of the self-assembled nanostructures. This result will be helpful for the design and fabrication of nanostructures of phthalocyanine and even porphyrin derivatives with novel morphologies. The star-shaped nanostructures were found to have better semiconducting properties than the ring-shaped nanostructures.

Experimental Section

Instrumentation: The ^1H NMR spectrum was recorded with a Bruker DPX 300 spectrometer (300 MHz) in $CDCl_3$ by using the residual solvent resonance of $CHCl_3$ at δ = 7.26 ppm relative to $SiMe_4$ as internal reference. The MALDI-TOF mass spectrum was recorded with a Bruker BIFLEX III ultra-high resolution Fourier transform ion cyclotron resonance (FT-ICR) mass spectrometer by using α-cyano-4-hydroxycinnamic acid as matrix. Electronic absorption spectra were obtained with a Hitachi U-4100 spectrophotometer; the ring-shaped nanostructures formed as a film were tested on a quartz plate, and the star-shaped nanostructures dispersed in methanol were tested in a quartz cuvette. Elemental analysis was performed with an Elementar Vavio El III. Fourier-transform infrared spectra were recorded in KBr pellets with 2 cm^{-1} resolution with an αALPHA-T spectrometer. Transmission electron microscopic images were recorded with a JEOL-100CX II electron microscope operating at 100 kV. Scanning electron microscopic images were obtained with a JEOL JSM-6700F electron microscope. For TEM imaging, the ring-shaped nanostructures formed as a film were transferred to a carbon-coated grid and for the star-shaped nanostructures a drop of sample solution was cast onto a carbon/copper grid. For SEM imaging, Au (1–2 nm) was sputtered onto these grids to prevent charging effects and to improve image clarity. X-ray diffraction was performed with a Rigaku D/max-cB X-ray diffractometer, the two types of nanostructures were tested in a silicon pellet.

Device Fabrication: The Au electrodes were thermally evaporated onto the ordered nanostructures by use of a micrometer-sized Au wire as the mask. These electrodes have an inter-electrode distance (*L*) of 55 μm. The current–voltage characteristics were obtained with a Keithley 4200 semiconductor characterization system at room temperature in air.

Chemicals: DMF and *n*-octanol were distilled from anhydrous $MgSO_4$ and sodium, respectively, under reduced pressure. The water used in the experiment was ultrapure. Column chromatography was carried out on silica gel (Qingdao Hailang, 200–300 mesh) with the indicated eluent. 4,5-Dichlorophthalonitrile was prepared according to published procedures.[27] All other chemicals and solvents were reagent grade and used as received without further purification.

Preparation of 4,5-Bis[3,5-bis(methoxycarbonyl)phenoxy]phthalonitrile (4): 4,5-Bis[3,5-bis(methoxycarbonyl)phenoxy]phthalonitrile (**4**) was prepared according to the following procedure: A mixture of 4,5-dichlorophthalonitrile (**2**; 1.0 g, 5.1 mmol), dimethyl 5-hydroxyisophthalate (**3**; 2.6 g, 12.2 mmol), and potassium carbonate (3.53 g, 25.5 mmol) in DMF (60 mL) was heated at 80 °C overnight. The solvent was then removed in vacuo. The residue was purified by silica gel chromatography using $CHCl_3$ as eluent to give **4** as a white solid (2.14 g, 77%).

Preparation of the Unsymmetrical (Phthalocyaninato)zinc Complex 1: Compound **1** was prepared according to a published procedure.[28] A mixture of compound **4** (55 mg, 0.1 mmol), phthalonitrile (115 mg, 0.9 mmol), $Zn(OAc)_2{\cdot}2H_2O$ (55 mg, 0.25 mmol), and DBU (500 mg) in octanol (5 mL) was heated at 150 °C under a slow stream of nitrogen overnight. After cooling to room temperature, the volatiles were removed in vacuo. The residue was dissolved in $CHCl_3$ and subjected to chromatography on a silica gel column with $CHCl_3/CH_3OH$ (99:1, v/v) as eluent. The first blue band containing **1** was collected, followed by another blue band containing a series of symmetrical and unsymmetrical (phthalocyaninato)zinc complexes according to mass spectrometric characterization,

which, however, could not be separated by general column chromatography at this stage despite great efforts. After removing the solvent in vacuo, the residue was again subjected to chromatography under similar conditions and then recrystallized from $CHCl_3$ and CH_3OH to give the target compound **1** as a blue solid (48 mg, 35%). ^1H NMR (300 MHz, $CDCl_3$): δ = 0.72–0.80 (m, 12 H), 1.14–1.26 (m, 32 H), 1.33 (br., 8 H), 1.69 (br., 8 H), 4.19 (br., 8 H), 7.46–7.54 (m, 8 H), 7.85 (br., 4 H), 8.15 (br., 2 H), 8.31 (br., 6 H) ppm. MS: calcd. for $C_{80}H_{88}N_8O_{10}Zn$ $[M + H]^+$ 1387.01; found 1387.2. $C_{80}H_{88}N_8O_{10}Zn{\cdot}C_2H_5OH$ (1433.08): calcd. C 68.72, H 6.61, N 7.82; found C 68.89, H 6.73, N 7.65.

Preparation of Nanoaggregates: The preparation of the two types of nanoaggregates are detailed in Scheme S2 (Supporting Information). The ring-shaped nanostructures were prepared by a simple one-step process at the chloroform/water interface.[29] During the evaporation of chloroform, self-assembled ordered films were formed driven by the compression force arising from the shrinking liquid/liquid interface. Upon complete evaporation of the solvent, a complete monolayer film was left on the water interface. The film was then transferred to a carbon-coated grid for TEM and SEM observation. The star-shaped nanostructures were prepared by the solution mixture method according to the following procedure.[30] Methanol (3 mL) was poured over a chloroform (1 mL) solution of compound **1** to form two layers. After allowing the solution to equilibrate at ambient temperature for 1 d, loose aggregates were clearly observed. These precipitates were then transferred to a carbon-coated grid by pipette for TEM and SEM observations. The experimental results were stable and reproducible under the experimental conditions described above.

Supporting Information (see footnote on the first page of this article): ^1H NMR spectrum of compound **1** in $CDCl_3$, MALDI-TOF mass spectrum of compound **1**, IR spectra of compound **1**, ring-shaped and star-shaped nanostructures of **1** in the region 400–4000 cm^{-1} with 2 cm^{-1} resolution, optimized molecular dimensions of compound **1**, self-assembly processes of the ring- and star-shaped nanostructures of compound **1**, electronic absorption spectroscopic data for compound **1** dissolved in $CHCl_3$, ring-shaped nanostructures of **1** as a film, and star-shaped nanostructures of **1** dispersed in methanol.

Acknowledgments

Financial support from the Natural Science Foundation of China and the Ministry of Education of China is gratefully acknowledged.

[1] F. Vögtle, *Supramolecular Chemistry*, Wiley, Chichester, **1991**.
[2] J.-M. Lehn, *Supramolecular Chemistry: Concepts and Perspectives*, VCH, Weinheim, **1995**.
[3] P. G. Schouten, J. M. Warman, M. P. de Haas, M. A. Fox, H. L. Pan, *Nature* **1991**, *353*, 736.
[4] J.-M. Lehn, *Science* **2002**, *295*, 2400.
[5] a) M. Yun, N. V. Myung, R. P. Vasquez, C. Lee, E. Menke, R. M. Penner, *Nano Lett.* **2004**, *4*, 419–422; b) H. Gan, H. Liu, Y. Li, Q. Zhao, Y. Li, S. Wang, T. Jiu, N. Wang, X. He, D. Yu, D. Zhu, *J. Am. Chem. Soc.* **2005**, *127*, 12452–12453.
[6] a) K. Balakrishnan, A. Datar, R. Oitker, H. Chen, J. Zuo, L. Zang, *J. Am. Chem. Soc. Chem.* **2005**, *127*, 10496–10497; b) K. Balakrishnan, A. Datar, T. Naddo, J. Huang, R. Oiker, M. Yen, J. Zhao, L. Zang, *J. Am. Chem. Soc.* **2006**, *128*, 7390–7398.
[7] X. Gong, T. Milic, C. Xu, J. D. Batteas, C. M. Drain, *J. Am. Chem. Soc.* **2002**, *124*, 14290–12491.
[8] a) J. M. Schnur, *Science* **1993**, *262*, 1669–1676; b) T. Shimizu, M. Masuda, H. Minamikawa, *Chem. Rev.* **2005**, *105*, 1401–1444; c) J. Hu, Y. Guo, H. Liang, L. Wan, L. Jiang, *J. Am. Chem. Soc.* **2005**, *127*, 17090–17095; d) M. Steinhart, R. B. Wehrspohn, U. Gösele, J. H. Wendorff, *Angew. Chem. Int. Ed.* **2004**, *43*, 1334–1344; e) Q. Liu, Y. Li, H. Liu, Y. Chen, X. Wang, Y. Zhang, X. Li, J. Jiang, *J. Phys. Chem. C* **2007**, *111*, 7298–7301.
[9] a) D. M. Vriezema, J. Hoogboom, K. Velonia, K. Takazawa, P. C. M. Christianen, J. C. Maan, A. E. Rowan, R. J. M. Nolte, *Angew. Chem. Int. Ed.* **2003**, *42*, 772–776; b) Y. Li, X. Li, H. Liu, S. Wang, H. Gan, J. Li, N. Wang, X. He, D. Zhu, *Angew. Chem. Int. Ed.* **2006**, *45*, 3639–3643.
[10] a) G. McDermott, S. M. Prince, A. A. Freer, A. M. Hawthormthwaite-Lawless, M. Z. Papiz, R. J. Cogdell, N. W. Isaacs, *Nature* **1995**, *374*, 517; b) A. P. H. J. Schenning, F. B. G. Benneker, H. P. M. Geurts, X. Y. Liu, R. J. M. Nolte, *J. Am. Chem. Soc.* **1996**, *118*, 8549–8552.
[11] a) A. B. P. Lever, C. C. Leznoff, *Phthalocyanine: Properties and Applications*, VCH, New York, **1989–1996**, vols. 1–4; b) N. B. McKeown, *Phthalocyanines Materials: Synthesis Structure and Function*, Cambridge University Press, New York, **1998**; c) K. M. Kadish, K. M. Smith, R. Guilard, *The Porphyrin Handbook*, Academic Press, San Diego, **2000–2003**, vols. 1–20; d) J. Jiang (Ed.), "Advances in Functional Phthalocyanine Materials" in *Structure and Bonding* (Series Ed.: D. M. P. Mingos), Springer, Heidelberg, **2010**, vol. 135.
[12] G. de la Torre, G. Botarri, U. Hahn, T. Torres, *Struct. Bonding (Berlin)* **2010**, *135*, 1–44.
[13] a) L. Wu, Q. Wang, J. Lu, Y. Bian, J. Jiang, X. Zhang, *Langmuir* **2010**, *26*, 7489–7497; b) W. Lv, X. Zhang, J. Lu, Y. Zhang, X. Li, J. Jiang, *Eur. J. Inorg. Chem.* **2008**, *27*, 4255–4261.
[14] D. M. Guldi, A. Gouloumis, P. Vázquez, T. Torres, V. Georgakilas, M. Prato, *J. Am. Chem. Soc.* **2005**, *127*, 5811–5813.
[15] W. Liu, T. J. Jensen, F. R. Fronczek, R. P. Hammer, K. M. Smith, M. G. H. Vicente, *J. Med. Chem.* **2005**, *48*, 1033–1041.
[16] a) R. Li, X. Zhang, P. Zhu, D. K. P. Ng, N. Kobayashi, J. Jiang, *Inorg. Chem.* **2006**, *45*, 2327–2334; b) Y. Bian, L. Li, J. Dou, D. Y. Y. Cheng, R. Li, C. Ma, D. K. P. Ng, N. Kobayashi, J. Jiang, *Inorg. Chem.* **2004**, *43*, 7539–7544.
[17] M. Kasha, H. R. Rawls, M. A. EI-Bayoumi, *Pure Appl. Chem.* **1965**, *11*, 371–392.
[18] a) F. Wurthner, *Chem. Commun.* **2004**, 1564–1579; b) P. M. Kazmaier, R. Hoffmann, *J. Am. Chem. Soc.* **1994**, *116*, 9684–9691; c) E. H. Hadicke, F. Graser, *Acta Crystallogr., Sect. C* **1986**, *42*, 189–195.
[19] S. Liu, G. Sui, R. Cormier, R. Leblanc, B. Gregg, *J. Phys. Chem. B* **2002**, *106*, 1307–1315.
[20] G. Klebe, F. Graser, E. Hadicke, J. Berndt, *Acta Crystallogr., Sect. B* **1989**, *45*, 69–77.
[21] F. Würthner, C. Thalacker, S. Diele, C. Tschierske, *Chem. Eur. J.* **2001**, *7*, 2245–2253.
[22] A. S. Gardberg, S. Yang, B. M. Hoffman, J. A. Ibers, *Inorg. Chem.* **2002**, *41*, 1778–1781.
[23] a) R. L. Judd, C. H. Lavdas, *J. Heat Transfer* **1980**, *102*, 461; b) O. I. Vinogradova, *Colloids Surf. A* **1994**, *82*, 247; c) L. A. Estevez, L. Z. Pino, I. A. Cavicchioli, E. Saez, *Chem. Eng. Commun.* **1991**, *105*, 231.
[24] X. Wang, Y. Zhang, X. Sun, Y. Bian, C. Ma, J. Jiang, *Inorg. Chem.* **2007**, *46*, 7136–7141.
[25] M. D. Porter, T. B. Bright, D. L. Allara, C. E. D. Chidseyin, *J. Am. Chem. Soc.* **1987**, *109*, 3559.
[26] a) Y. Che, A. Datar, K. Balakrishnan, L. Zang, *J. Am. Chem. Soc.* **2007**, *129*, 7234–7235; b) Y. Che, A. Datar, X. Yang, T. Naddo, J. Zhao, L. Zang, *J. Am. Chem. Soc.* **2007**, *129*, 6354–6355; c) P. Ma, Y. Chen, Y. Bian, J. Jiang, *Langmuir* **2010**, *26*, 3678–3684.
[27] A. Lux, G. G. Rozenberg, K. Petritsch, S. C. Moratti, A. B. Holmes, R. H. Friend, *Synth. Met.* **1999**, *102*, 1527–1528.
[28] M. Bai, P. C. Lo, J. Ye, C. Wu, W. P. Fong, D. K. P. Ng, *J. Porphyrins Phthalocyanines* **2006**, *10*, 548 (Fourth International Conference on Porphyrins and Phthalocyanines, Rome).

[29] C. Zhang, X. Zhang, X. Zhang, X. Ou, W. Zhang, J. Jie, J. C. Chang, C. S. Lee, S. T. Lee, *Adv. Mater.* **2009**, *21*, 4172–4175.
[30] a) W. Su, Y. Zhang, C. Zhao, X. Li, J. Jiang, *ChemPhysChem* **2007**, *8*, 1857–1862; b) G. Lu, X. Zhang, X. Cai, J. Jiang, *J. Mater. Chem.* **2009**, *19*, 2417–2424; c) X. Gong, T. Milic, C. Xu, J. D. Batteas, C. M. Drain, *J. Am. Chem. Soc.* **2002**, *124*, 14290–14291; d) G. Lu, Y. Chen, Y. Zhang, M. Bao, Y. Bian, X. Li, J. Jiang, *J. Am. Chem. Soc.* **2008**, *130*, 11623–11630; e) Y. Gao, X. Zhang, C. Ma, X. Li, J. Jiang, *J. Am. Chem. Soc.* **2008**, *130*, 17044–17052.

Received: October 17, 2010
Published Online: February 15, 2011

